

# Eucalyptus Kraft Pulp Fibers as an Alternative Reinforcement of Silicone Composites. II. Thermal, Morphological, and Mechanical Properties of the Composites

S. U. A. Redondo, M. C. Gonçalves, I. V. P. Yoshida

*Instituto de Química, Universidade Estadual de Campinas, CP 6154, 13083-970, Campinas, São Paulo, Brazil*

Received 11 June 2002; accepted 26 October 2002

**ABSTRACT:** Silicone composites reinforced with short eucalyptus pulp fibers were obtained. The composites were prepared with untreated fibers and with fibers modified with a silane coupling agent, vinyltriethoxysilane, with tetrahydrofuran or ethanol as a solvent. The surface treatment improved the adhesion at the fiber–matrix interface, and vinyltriethoxysilane was suitable for forming a covalent and nonhydrolyzed interface in the composites. The thermal stability of the composites was lower than

that of the silicone matrix, with a distinct mechanism of degradation, because of the presence of the cellulosic fibers in the composite. The tensile properties of the composites depended more on the fiber dispersion in the matrix than on the nature of the interface. © 2003 Wiley Periodicals, Inc. *J Appl Polym Sci* 89: 3739–3746, 2003

**Key words:** silicones; networks; fibers

## INTRODUCTION

Silicone materials have long been known for their unique properties, such as their low-temperature flexibility, chemical inertness, water repellency, and biocompatibility.<sup>1,2</sup> In general, silicone-crosslinked networks show poor mechanical properties. Therefore, the use of reinforcing fillers to improve these properties is necessary.<sup>3,4</sup> In these materials, excellent mechanical performance has been achieved with hydrophobic silica as a filler.<sup>1,4</sup> Moreover, composites based on natural fibers such as jute,<sup>5</sup> pineapple,<sup>6</sup> sisal,<sup>7</sup> coconut,<sup>8</sup> and wood,<sup>9</sup> used as reinforcing elements in several synthetic organic polymer matrices such as polyethylene, polypropylene, polyurethane, and polyester resins, are receiving considerable attention nowadays.<sup>7,9,10</sup> Natural fibers are usually cheaper than inorganic fillers such as silica, glass fibers, and mica.<sup>11</sup> Although the mechanical properties of cellulosic fibers are poor in relation to inorganic fillers, they offer a number of advantages, such as their renewable, non-toxic and nonabrasive character, low density, and biodegradability.<sup>6,7,12</sup>

Hydrophilic cellulosic fibers are generally incompatible with hydrophobic polymeric matrices, and this causes poor adhesion between the fibers and matrices<sup>9</sup> and makes the dispersion of the fibers in the polymeric matrices difficult.<sup>13,14</sup> As described by Gatenholm et al.,<sup>13</sup> who studied composites of cellulosic fibers with polypropylene, polyethylene, and polystyrene, the bad dispersion of fibers results in their agglomeration into knotty masses, leading to composites with poor final properties. Despite this, natural fibers can be used as an alternative filler after appropriate modifications on their surfaces. For better interactions at the fiber–matrix interface, several chemical treatments on fiber surfaces have been used, such as low-molecular-weight polymer pretreatments, acetylation, and reactions with isocyanate and silane coupling agents.<sup>11,14–16</sup> In this article, the results of the investigation on the effect of eucalyptus kraft pulp fibers as an alternative reinforcement element in a silicone polymeric network are reported. Part I of this study describes the characterization and chemical modification of these fibers with vinyltriethoxysilane (VTES).<sup>17</sup>

## EXPERIMENTAL

### Materials

Poly(methylsiloxane) [PMS; number-average molecular weight ( $M_n$ ) = 5096/mol], vinyl-functionalized poly(dimethylsiloxane) (PDMS-Vi;  $M_n$  = 13,900/mol), and 1,3,5,7-tetramethyl,1,3,5,7-tetravinylcyclotetrasiloxane ( $D_4^V$ ) were supplied by Dow Corning (Horto-

Correspondence to: I. V. P. Yoshida (valeria@iqm.unicamp.br).

Contract grant sponsor: Fundação de Amparo à Pesquisa do Estado de São Paulo; contract grant number: 95/03636-3 and 99/05491-3.

lândia, SP, Brazil). The platinum divinyltetramethyl-disiloxane complex (platinum catalyst, 3–3.5% platinum concentration in PDMS-Vi) was supplied by Gelest (Karlsruhe, Germany). The eucalyptus kraft pulp fibers were supplied by Companhia Suzano de Papel e Celulose (Suzano, SP, Brazil).

### Compounding procedure

Three sets of composite materials were obtained: the first set with untreated cellulosic fibers, named CFP, and the other two with cellulosic fibers modified with 20% VTES. In the last two sets of composites, the modification reaction performed on the fiber surface was carried out in tetrahydrofuran (THF) or ethanol (EtOH) as a solvent, as described in part I of this study.<sup>17</sup> These composite samples were named CVST and CVSEt, respectively. The silicone matrix was obtained with a platinum-catalyzed hydrosilylation reaction of a mixture of PMS, D<sub>4</sub><sup>Y</sup>, and PDMS-Vi in a 7.5:2.5:90 (w/w/w) ratio. The matrix and cellulosic fibers were mixed in a mechanical mixer, and this was followed by compression molding at 60°C for 1 h under 3.5–4 tons of pressure. After the molding, the samples were subjected to annealing at 50°C for 16 h to complete the cure reaction. Each composite set was prepared with 10 and 20 wt % cellulosic fibers.

### Morphological analysis

The fiber–matrix interface was studied by field emission scanning electron microscopy (FESEM) with a JM-6304F microscope (JEOL, Tokyo, Japan) operated

at 5 kV on a cryogenic fracture surface coated with gold. The dispersion of fibers into the matrix was observed by optical microscopy with an SZ-BR stereomicroscope (Olympus, Tokyo, Japan).

### Thermal properties

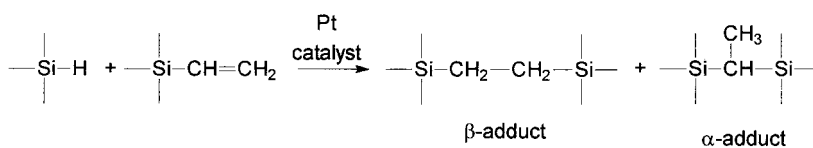
The thermogravimetric analysis (TGA) of composite materials was carried out in a TA 2950 thermobalance (TA Instruments, New Castle, DE) in the range of 30–1000°C at a scanning rate of 20°C/min under an argon flow. The samples were also analyzed by differential scanning calorimetry with a 2910 DSC (TA Instruments) at a scanning rate of 10°C/min in the range of –150 to +150°C.

### Mechanical testing

The tensile properties were determined according to ASTM D 412, with an EMIC 2000 tensile tester (São José dos Pinhais, PR, Brazil), with a 500-N load cell and a crosshead speed of 5 mm/min. All mechanical tests were evaluated with at least five test specimens for each composition. Specimens were conditioned at 23°C and 50% relative humidity for 24 h before the testing.

## RESULTS AND DISCUSSION

The silicone matrix was obtained by a platinum-catalyzed hydrosilylation reaction, which corresponded to an addition reaction of a hydride silane to carbon–carbon multiple bonds, giving rise mainly to  $\beta$  adducts:



The modification of the cellulosic fiber surface with VTES allowed the presence of vinyl groups on the fiber surface. Then, these groups could also react with Si–H bonds from the silicone-forming matrix through the same hydrosilylation reaction, and this allowed the formation of covalent bonds between the fiber coating and the matrix, as can be seen in the simplified scheme illustrated in Figure 1. The formation of Si–C bonds, mainly ethylene bridges, at the fiber–matrix interface enhanced the adhesion and the stress transfer between the matrix and the fiber.<sup>12</sup>

The cryogenic fracture surfaces of the composite samples were analyzed by FESEM. As can be seen in Figure 2(a), in the untreated-fiber composites, there was a lack of adhesion between the fibers and silicone matrix, shown by the pullout of the former. Neverthe-

less, in some regions of this sample, an interaction at the fiber–matrix interface could be observed, as shown in Figure 2(b). This photomicrograph shows the fiber and matrix were fractured together, and no pullout was observed. This could be attributed to two main factors: first, the low surface tension of silicone polymers, which allowed these polymers to wet the fiber surface, and second, the possibility of SiH groups from PMS reacting with the hydroxyl groups from the fiber surface through the following reaction:



When fibers were modified with the silane coupling agent, the adhesion at the fiber–matrix interface was

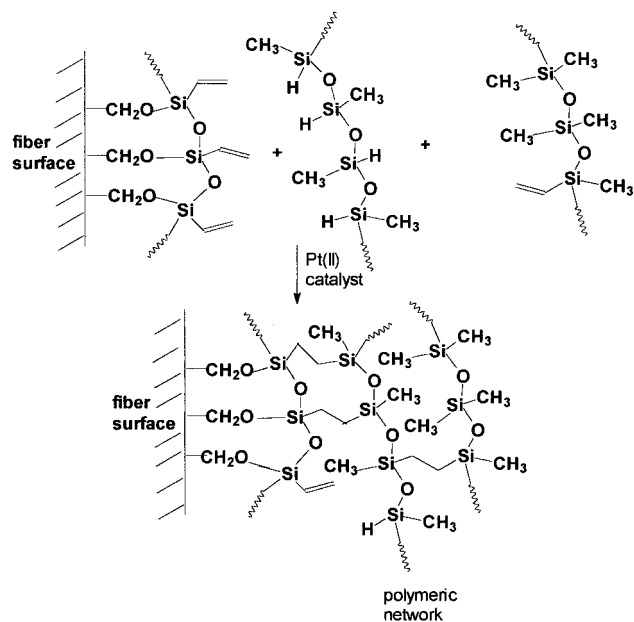


**Figure 1** Scheme of the cure reaction of a silicone matrix in the presence of modified cellulosic fibers.

significantly improved, as can be seen in Figure 2(c,d). The former photomicrograph shows that the fiber-matrix interface did not fail during the cryogenic frac-

ture. This fracture occurred almost exclusively in the matrix and perpendicularly to the fiber direction. On the basis of these results, it was possible to conclude that the silane VTES was a good adhesion promoter between the fibers and the hydrophobic silicone matrix, notwithstanding the solvent used in the modification reaction.

**Dispersion behavior of the fibers in the matrix**

The optical micrography of the CFP10 composite, prepared by a dispersion of 10 wt % untreated cellulosic fibers in the silicone matrix, can be seen in Figure 3(a). It was not possible to make a homogeneous dispersion of untreated fibers in the matrix, and this led to agglomerates of fibers in the cured silicone matrix. Through FESEM image analysis of the fracture surface of this composite (Fig. 4), the presence of two distinct regions was observed: (1) fiber-rich regions, in which the fibers were not well encapsulated by the silicone matrix, and (2) regions without fibers inside the matrix. The hydrophilic character of the cellulosic fibers was responsible for the nonuniform distribution of fibers in the hydrophobic matrix, which led to the presence of agglomerations in knotty masses, similar

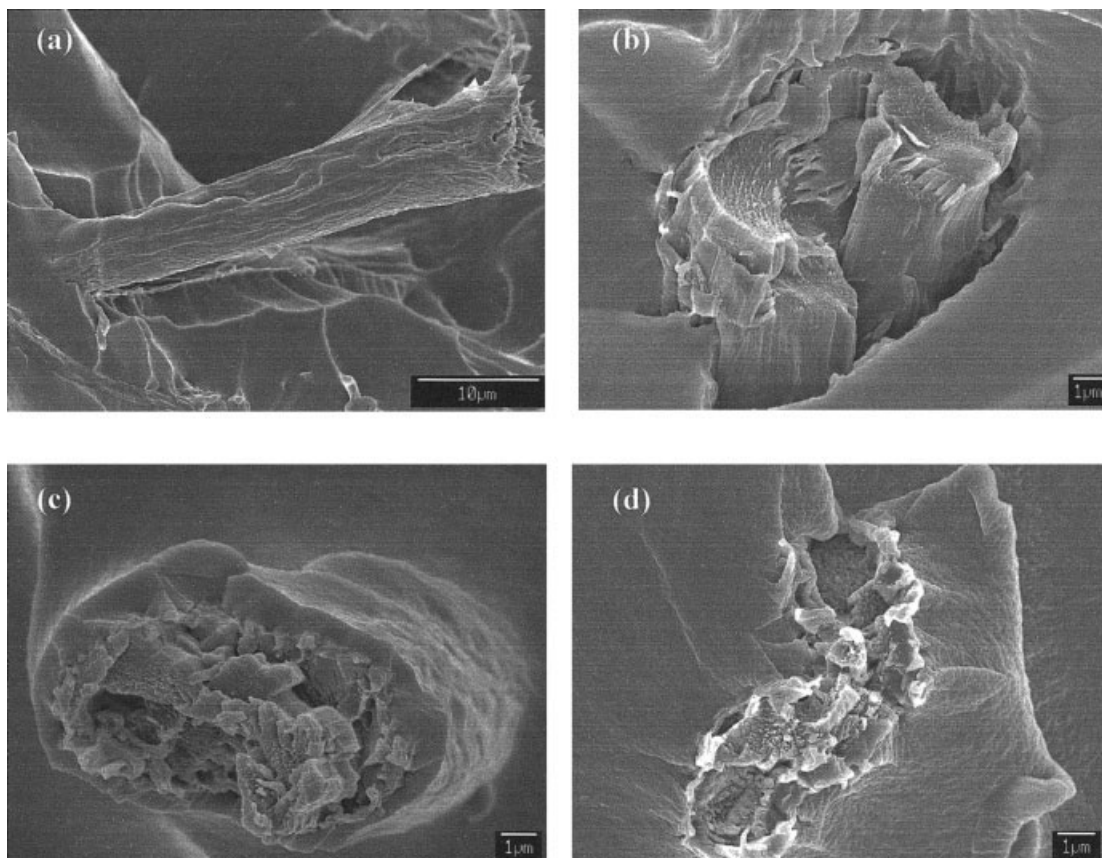
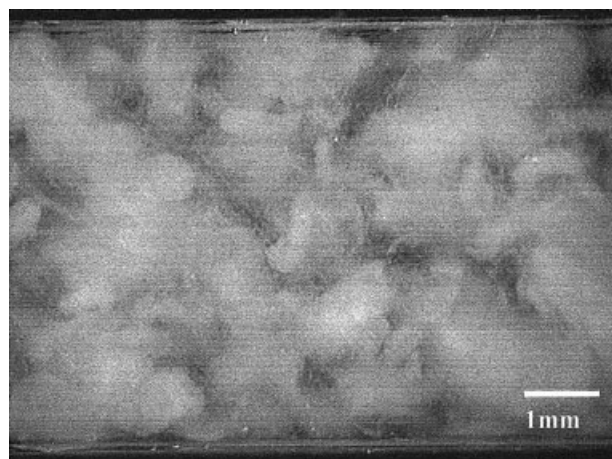
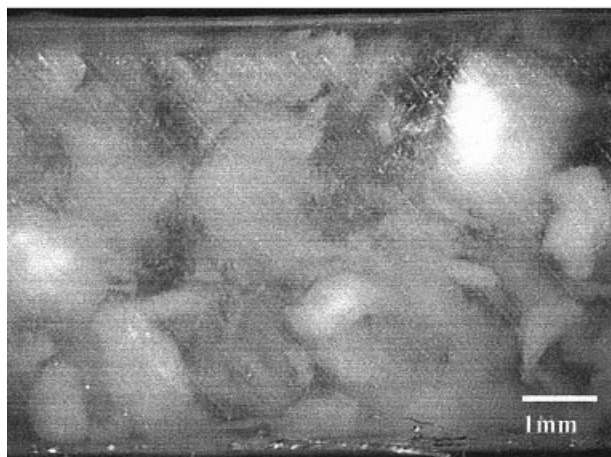


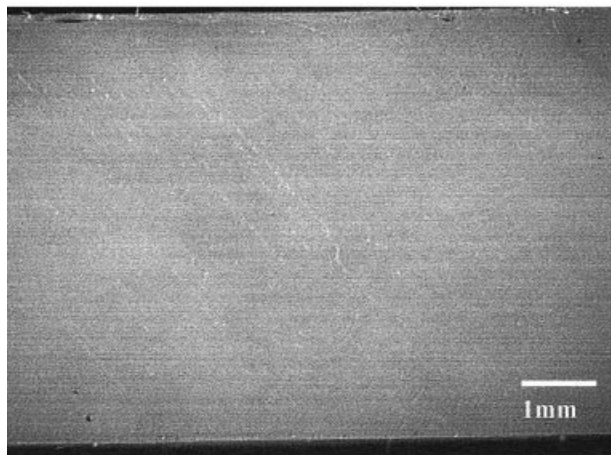
**Figure 2** FESEM photomicrographs of the composites: (a,b) untreated fibers, (c) VTES/THF-modified fibers, and (d)VTES/EtOH-modified fibers.



(a)



(b)



(c)

**Figure 3** Optical micrographs of the composites: (a) CFP10, (b) CVST10, and (c) CVSEt10 (magnification, 10 $\times$ ).

to the description made by Gatenholm et al.<sup>13</sup> for polyolefin/cellulosic fiber composites. The fibers tended to associate among themselves because of the

hydrogen bonding performed by the hydroxyl groups on the fiber surface.<sup>8</sup>

The composites obtained with cellulosic fibers modified with VTES/THF also showed bad dispersion behavior, with fibers forming bundles in the silicone matrix, as shown in Figure 3(b), with agglomeration similar to that of the untreated-fiber composite. However, composites prepared with fibers modified in VTES/EtOH showed significantly better results in the dispersion of fibers in the matrix for both composite compositions [Fig. 3(c)].

The difference in the dispersion of fibers in the matrix was associated with the modification reaction step. In part I of this study,<sup>17</sup> it is reported that a better dispersion of fibers during the modification reaction was reached when EtOH was used as a solvent because of its better ability to solvate the cellulosic fibers than THF. After the modification reaction, the VTES/THF fibers stood together, whereas the VTES/EtOH fibers were loose. This last treatment was responsible for the reduction of the hydrogen-bonding interactions among the fibers that held them together. Therefore, the efficacy of the dispersion of the fibers in the modification reaction determined the quality of the distribution of fibers in the silicone matrix during the compounding procedure.

### Thermal behavior

TGA curves obtained for the silicone matrix and composites in flowing argon are shown in Figure 5(a). The silicone matrix showed good thermal stability, with an initial temperature of weight loss above 350°C. Two distinct steps of thermal degradation were observed: the first with the temperature of the maximum rate of degradation ( $T_{\max}$ ) at 475°C and the second with  $T_{\max}$  around 696°C, as can be seen in Figure 5(b).

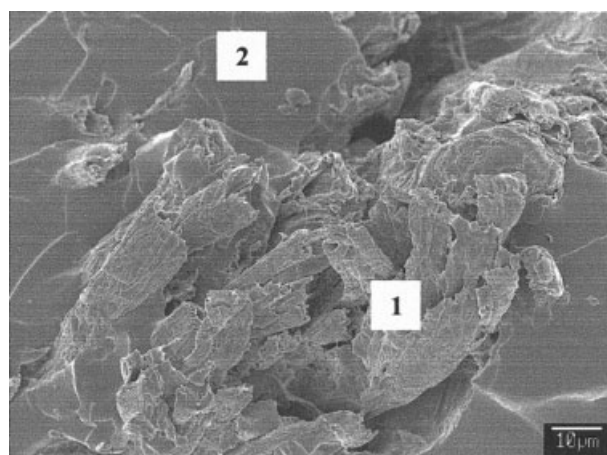
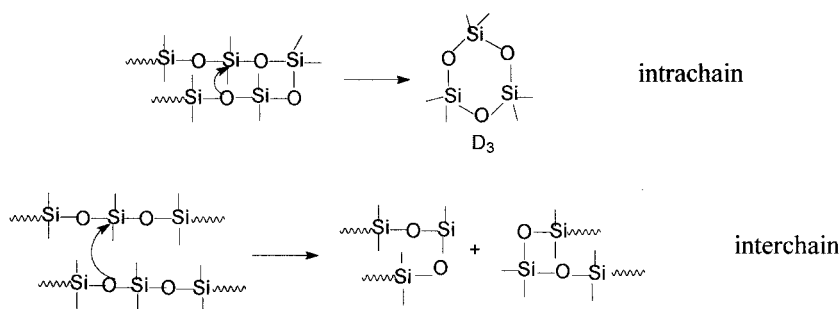


**Figure 4** FESEM photomicrograph of the CFP10 composite: (1) fiber-rich region; (2) matrix without fibers.

The thermal degradation of linear silicones in an inert atmosphere is mainly governed by thermal depolymerization, which involves the siloxane backbone. Poly(dimethylsiloxane) (PDMS) depolymerizes completely and does not form a solid residue. The

mechanism of this depolymerization is based on the interchain and intrachain reactions, producing volatile linear and cyclic oligomers, such as  $D_3$  and  $D_4$ . In linear PDMS with  $\text{Si}(\text{CH}_3)_2\text{OH}$  end groups, this depolymerization is accelerated.<sup>18</sup>



In polysiloxane networks with linear segments between nodes, similar to the silicone matrix used in this study, the initial weight loss was also attributed to the depolymerization with the evolution of volatile siloxane oligomers. Contrary to linear silicone, this step corresponded to a 15% weight loss in the silicone matrix. Above 600°C, a mineralization process occurred, producing silicon oxycarbides residues ( $\text{SiC}_x\text{O}_{4-x}$ ).<sup>19,20</sup>

TGA curves of the composites also showed two stages of thermal decomposition. The first in the 270–360°C range was attributed to the degradation of the cellulosic fibers, and the second and main stage, with  $T_{\text{max}}$  in the 480–540°C range, was associated with the silicone-matrix degradation. In these composites, the presence of cellulosic fibers led to a decrease in the thermal stability of the composite material, compared with that of the pure silicone matrix, because of the lower degradation temperature of eucalyptus fibers.<sup>17</sup> Similar behavior was also observed by Albano et al.<sup>7</sup> in polyolefin/sisal composites. The pure silicone matrix showed two steps of thermal degradation with similar weight loss percentages. After the introduction of fibers, the main step of weight loss occurred in the same temperature range as the first step, from 480 to 540°C, as could be seen in the derived of TGA curves in Figure 5(b).

The activation energy ( $E_a$ ) value of each degradation step of the silicone matrix was determined with the dynamic method derived by Ozawa.<sup>21</sup> The mean  $E_a$  value of the first thermal degradation step for this silicone matrix was 156.6 kJ/mol, and the mean  $E_a$  value of the second was 258.6 kJ/mol.<sup>20</sup> In the CVSEt10 composite, the degradation of the silicone matrix corresponding to  $T_{\text{max}} = 479^\circ\text{C}$  presented a mean  $E_a$  value of 76 kJ/mol, as determined by the same procedure. This effect could be associated with the presence of acids and alcoholic byproducts in the composite, produced in the first step of the decomposition process, attributed to cellulosic fibers,<sup>22</sup> which accel-

erated the degradation of the siloxane main chain. A similar effect was observed in several studies in which the thermal degradation process of polysiloxanes was changed by the presence of ionic impurities, which led

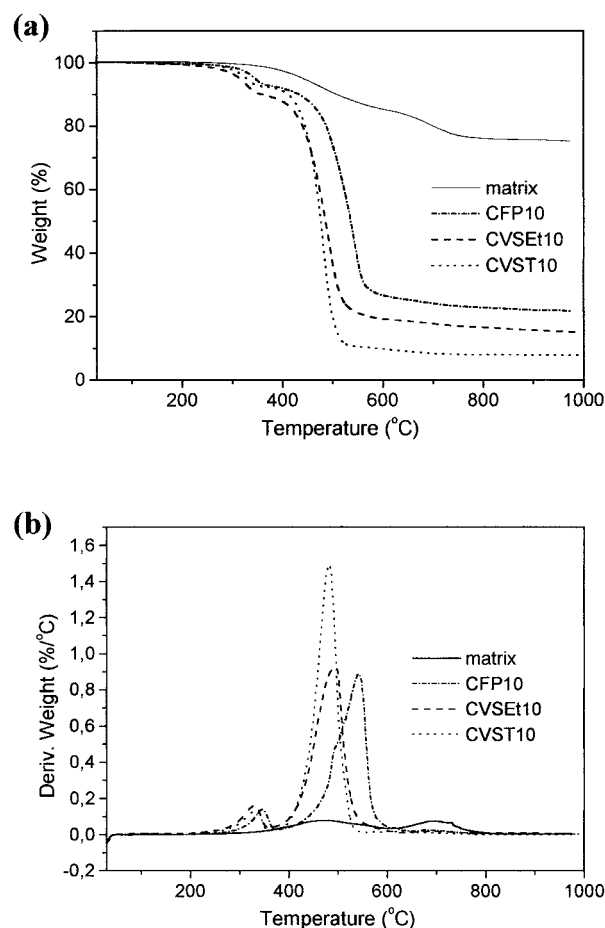


**Figure 5** TGA curves of the untreated-fiber and modified-fiber composites and the silicone matrix: (a) the weight (%) as a function of temperature and (b) the derived weight (%/°C) as a function of temperature.

TABLE I  
Mechanical Properties of Silicone/Eucalyptus Fiber Composites

Sample	Fiber content (%)	Tensile strength (MPa)	Modulus (MPa)	Elongation at break (%)
Matrix	0	0.49 (0.03)	5.75 (0.29)	10.3 (1.05)
CFP10	10	0.50 (0.04)	6.84 (1.01)	7.87 (1.0)
CFP20	20	0.63 (0.09)	12.28 (0.94)	6.41 (1.01)
CVST10	10	0.58 (0.05)	6.89 (0.49)	9.11 (1.34)
CVST20	20	0.61 (0.06)	11.08 (1.3)	7.22 (0.30)
CVSEt10	10	1.04 (0.09)	13.52 (0.65)	9.72 (0.8)
CVSEt20	20	1.23 (0.13)	17.6 (0.63)	9.1 (1.23)

SD are given in parentheses

to the acceleration of Si—O cleavage and the cyclization process of the chain.<sup>23</sup>

The percentages of the residues in the pyrolytic process of the composites at 800°C were lower than those of the pure silicone matrix, varying from 23% for CFP10 to 8% for CVST10. These were the result of the difference in the local fiber concentration due to the heterogeneities in the distribution of fibers inside the matrix.

The glass-transition temperatures of the silicone matrix and the composites was determined by DSC experiments and was observed to be around -120°C. The glass-transition temperatures of the composites were not significantly affected by the presence of fibers.

### Tensile tests

The effect of the introduction of fibers on the mechanical properties of the silicone network was analyzed by tensile tests, and the results are summarized in Table I. Typical comparative stress-strain curves of the silicone matrix and composite samples are shown in Figure 6.

The silicone network showed poor tensile properties, mainly because of the relatively low molecular

weight of the precursor polymers. When fibers were modified with THF as a solvent, the tensile test results showed that the presence of VTES did not impart significant changes in the tensile strength, in comparison with the untreated-fiber composites, despite the increase in the adhesion observed in the fiber-matrix interface. This behavior is better illustrated in Figure 7(a).

The heterogeneous distribution and the tendency of fiber agglomeration, even after the modification reaction, had a prominent effect in promoting stress concentrations and could mask the efficacy of the stress-transfer process between the silicone matrix and fibers through the Si—C interface. Therefore, these factors outweighed the performance of the VTES modification in improving the compatibility between the fibers and the silicone network. Similar results were obtained by Rozman et al.,<sup>8</sup> who studied coconut fiber/polypropylene composites compatibilized by lignin. According to Herrera-Franco and Aguilar-Veja,<sup>16</sup> composite materials based on short fibers or particles present problems that make the prediction of their effective mechanical properties difficult. The most common problems arise from the uneven distribution and orientation of fibers inside the matrix.

However, a significant improvement in the tensile strength was observed for CVSEt composites in comparison with the pure silicone matrix, with increases of 103 and 139% for CVSEt10 and CVSEt20, respectively. The surface topography of the modified fibers in EtOH were rougher than the untreated and VTES/THF-modified fibers, as presented in the previous work.<sup>17</sup> This surface characteristic can also improve the adhesion at the interface by mechanical anchoring. It is known that fiber-matrix adhesion and the stress-transfer efficiency of the interface play an important role in determining the strength of a composite.<sup>5,6</sup> Therefore, in the CVSEt composites, the better distribution of fibers and the silane covalent-bonded in the fiber-matrix interface could facilitate the effective transfer of mechanical stress between them.<sup>11</sup> However, the bad distribution of fibers in the CFP and CVST samples did not allow the analysis of the silane

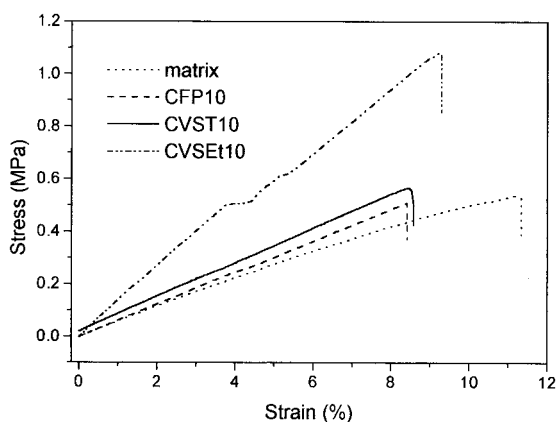
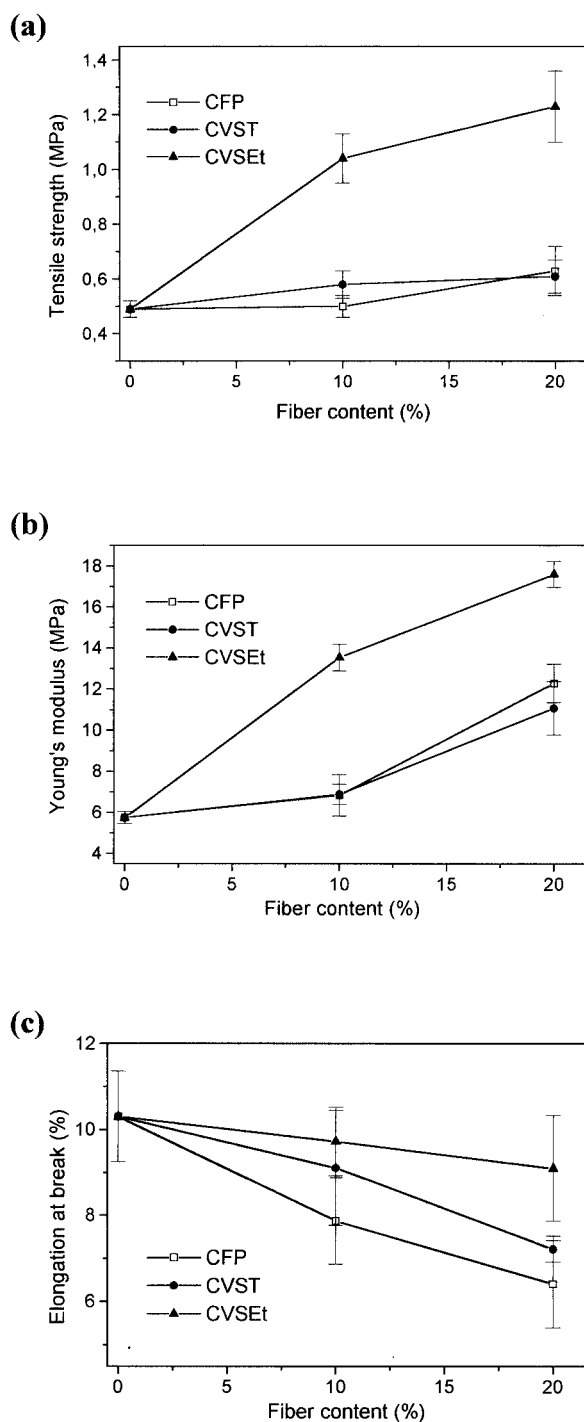


Figure 6 Typical stress-strain curves of the silicone matrix and CFP10, CVST10, and CVSEt10 composites.



**Figure 7** Effect of the fiber content on the variation of (a) the tensile strength, (b) Young's modulus, and (c) the elongation at break of silicone/eucalyptus-fiber composites.

adhesion effect by means of comparison with the CVSEt composite.

The increase in the tensile strength with the addition of 10 wt % fibers was 103%, whereas with the addition of 20 wt % fibers, the increase was only 18%. These results reflected the fiber-to-fiber interactions at high fiber loadings,<sup>6</sup> which did not contribute to an effective stress transference in the composite.

Figure 7(b) shows that Young's modulus presented a low increase with the introduction of 10 wt % untreated and VTES/THF-treated fibers. In composites with 20 wt % of these fibers, the increment was greater. The CVSEt composites showed a higher increase in the modulus value with the fiber loading than the other composites, probably because of the better distribution of fibers inside the matrix. The increase observed in the modulus indicated that the fibers imparted some stiffness to the matrix.

The curves of the elongation at break versus the fiber content are shown in Figure 7(c). In comparison with the unfilled silicone matrix, a decrease in the elongation was observed with an increase in the fiber content because of restrictions imposed by the filler.<sup>12</sup> This is a common observation with almost all filled composites.<sup>8,13</sup> The elongations observed in this pure silicone network were not large because of the relatively low molecular weights of the precursor polymers. However, CVSEt composites presented a lower decrease than the others. In the CFP and CVST composites, the nonuniform distribution of fibers promoted the break of the materials at low elongations.

## CONCLUSIONS

The modification of the cellulosic fiber surface by the VTES silane coupling agent significantly improved the adhesion at the fiber/silicone-matrix interface. However, the composites obtained with VTES/THF-modified fibers and untreated-fiber composites showed similar properties, and this was explained by the irregular distribution of fibers in the matrix. In the VTES/EtOH composites, a better dispersion of fibers in the silicone matrix was achieved, with a significant improvement in the tensile strength compared with that of the pure silicone matrix. Eucalyptus fiber/silicone composites showed a glass-transition temperature similar to that of the silicone matrix, at  $-120^{\circ}\text{C}$ . The presence of fibers in the silicone matrix accelerated its degradation mechanism.

## References

- Gu, Q. G.; Zhou, Q. L. *Eur Polym J* 1998, 34, 1727.
- Cush, R. J.; Winnan, H. W. In *Developments in Rubber Technology—Synthetic Rubbers*; Whelan, A.; Lee, K. S., Eds.; Applied Science: London, 1981; Vol. 2, Chapter 7, p 203.
- Osman, M. A.; Atallah, A.; Müller, M.; Suter, U. W. *Polymer* 2001, 42, 6545.
- Cochrane, H.; Lin, C. S. *Rubber Chem Technol* 1993, 66, 48.
- Saha, A. K.; Das, S.; Basak, R. K.; Bhatta, D.; Mitra, B. C. *J Appl Polym Sci* 2000, 78, 495.
- George, J.; Bhagawan, S. S.; Prabhakaran, N.; Thomas, S. *J Appl Polym Sci* 1995, 57, 843.
- Albano, C.; Gonzalez, J.; Ichazo, M.; Kaiser, D. *Polym Degrad Stab* 1999, 66, 179.
- Rozman, H. D.; Tan, K. W.; Kumar, R. N.; Abubakar, A.; Ishak, Z. A. M.; Ismail, H. *Eur Polym J* 2000, 36, 1483.

9. Rials, T. G.; Wolcott, M. P.; Nassar, J. M. *J Appl Polym Sci* 2001, 80, 546.
10. Hassan, M. L.; Nada, A. M. A. *J Appl Polym Sci* 2001, 80, 2018.
11. Josef, K.; Thomas, S.; Pavithran, C. *Polymer* 1996, 37, 5139.
12. Rana, A. K.; Mandal, A.; Mitra, B. C.; Jacobson, R.; Rowell, R.; Banerjee, A. N. *J Appl Polym Sci* 1998, 69, 329.
13. Gatenholm, P.; Bertilsson, H.; Mathiasson, A. *J Appl Polym Sci* 1993, 49, 197.
14. Ishak, Z. A. M.; Aminullah, A.; Ismail, H.; Rozman, H. D. *J Appl Polym Sci* 1998, 68, 2189.
15. Hill, C. A. S.; Khalil, H. P. S. A. *J Appl Polym Sci* 2000, 78, 1685.
16. Herrera-Franco, P. J.; Aguilar-Veja, M. J. *J Appl Polym Sci* 1997, 65, 197.
17. Redondo, S. U. A.; Radovanovic, E.; Gonçalves, M. C.; Yoshida, I. V. P. *J Appl Polym Sci* 2002, 85, 2573.
18. Thomas, T. H.; Kendrick, T. C. *J Polym Sci Part A-2: Polym Phys* 1969, 7, 537.
19. Radovanovic, E.; Gozzi, M. F.; Gonçalves, M. C.; Yoshida, I. V. P. *J Non-Cryst Solids* 1999, 248, 31.
20. Schiavon, M. A.; Redondo, S. U. A.; Pina, S. R. O.; Yoshida, I. V. P. *J Non-Cryst Solids* 2002, 304, 92.
21. Ozawa, T. *Bull Chem Soc Jpn* 1965, 38, 1881.
22. Statheropoulos, M.; Liodakis, S.; Tzamtzi, N.; Papa, A.; Kyriakou, S. *J Anal Appl Pyrolysis* 1997, 43, 115.
23. Ikeda, M.; Nakamura, T.; Nagase, Y.; Ikeda, K.; Sekine, Y. *J Polym Sci Polym Chem Ed* 1981, 19, 2595.